(To be presented at the International
Conference on Low and Intermediate Energy
Electromagnetic Interactions, Dubna,
U.S.S.R., 1967)

HEPL - 484
SLAC-PUB-266
JANUARY 1967

COHERENT PHOTOPRODUCTION OF THE η^o MESON FROM DEUTERIUM*

R. L. Anderson

Stanford Linear Accelerator Center

R. Prepost†

Department of Physics and High Energy Physics Laboratory

Stanford University

Stanford, California

* Work supported in part by the U. S. Office of Naval Research, Contract [Nonr 225(67)] and in part by the U. S. Atomic Energy Commission.

† Now at Stanford Linear Accelerator Center, Stanford University, Stanford, California.

Coherent Photoproduction of the η^{o} Meson from Deuterium

R. L. Anderson
Stanford Linear Accelerator Center

and

R. Prepost[†]

Department of Physics and High Energy Physics Laboratory

Stanford University

Stanford, California

INTRODUCTION

We have measured the differential cross section for the reaction $\gamma + D \rightarrow \eta^{o} + D$ near 90^{o} in the center of mass system from threshold to 150 MeV above threshold in approximately 20 MeV steps. These measurements have been made using counter techniques at the Stanford University 1.1 GeV linear electron accelerator.

The eta is a pseudoscalar meson with positive G parity and mass 548.6 ± 0.4 MeV. The process $\gamma + p \rightarrow \eta^{o} + p$ has been studied near threshold in a related experiment[1] and studies of the reaction $\gamma + D \rightarrow \eta^{o} + D$ will complement this information. Since both the deuteron and the eta meson are isoscalar particles only the isoscalar part of the $\langle \eta^{o} N | j_{\mu} | N \rangle$ matrix element may contribute to the coherent production from the deuteron.

EXPERIMENTAL APPARATUS

Observations of η^{o} production in the reaction $\gamma + D \rightarrow \eta^{o} + D$ has been accomplished by detecting the recoil deuteron. Since this process has a two-body final state, a measurement of the deuteron momentum and angle is sufficient to uniquely determine the incident photon energy. The experimental arrangement is shown in Fig. 1. The electron beam is brought out into the experimental end station and passes through three secondary emission monitors, a beam position monitor, and a fast torroid. The electron beam itself consists of pulses occurring at 23.0 Mc/sec, each less than 1 nsec in width during an overall machine pulse width of 1 μsec. This "chopped" beam is prepared by passing the electron beam between a set of plates near the accelerator gun to which an 11.5 Mc/sec rf voltage is applied. Immediately after the deflection plates, a collimator is positioned on the accelerator axis thus producing the "chopped" beam. This time structure in the beam is then used for a time of flight time marker in order to measure the time of flight distribution of particles traversing the spectrometer.

The electron beam passes through a 0.03 radiation length foil and is then deflected by a sweeping magnet. After collimation, the photon beam then passes through a liquid deuterium target. The beam position is monitored once more after the deuterium target, and then the photon beam energy is measured in a secondary emission quantameter.

The spectrometer is a 44 in. radius, 90^{o} bend, n=0 type magnet which is capable of 0.1% momentum resolution up to 700 MeV/c. The detecting counters consist of 7 1% momentum defining counters, and two focal plane defining counters.

Deuterons are identified by range, energy loss, and time of flight requirements. Under most experimental conditions the proton flux was some 100 times more intense than the deuteron flux. A typical time of flight distribution is shown in Fig. 2 for particles which have already been selected by range and energy loss. Under normal experimental conditions, the time of flight is set for deuterons, and the resultant deuteron signal has less than a 1% proton contamination.

EXPERIMENTAL PROCEDURE

The procedure used for the cross section measurements is similar to that used by R. Prepost, D. Lundquist, and D. Quinn[1] to measure the cross section for $\gamma + p \rightarrow \eta^{o} + p$. For a fixed spectrometer momentum and angle setting, the deuteron yield is measured as a function of primary electron energy. As the electron energy increases (i.e., the bremsstrahlung end point energy) the counter yields will increase when the threshold energy for a new process is reached. In particular, if the process has a two-body final state, the counter yields will rise at the threshold energy and trace out a bremsstrahlung curve for fixed photon energy and variable end point energy. This yield reaches an approximately constant value some 30 MeV above the threshold for the reaction. On the other hand, if the reaction has a three body final state such as $\gamma + D \rightarrow \pi^{+} + \pi^{-} + D$, then a measurement of the deuteron momentum and angle is not sufficient to identify the photon energy, and the yield continues to rise above the threshold with a contribution from all photon energies from the laboratory threshold energy to the bremsstrahlung end point energy. Our procedure has been to trace out the deuteron yield as a function of energy from the threshold for $\gamma + D \rightarrow \pi^{0} + D$ to approximately 150 MeV above the threshold for $\gamma + D \rightarrow \eta^{0} + D$. Figures 3 and 4 are two examples of such yield curves which show a signal due to $\gamma + D \rightarrow \pi^{0} + D$. The process $\gamma + D \rightarrow \gamma + D$ is too small to be seen against the much larger signal from $\gamma + D \rightarrow \pi^{0} + D$. The energy interval steps are approximately 10 MeV and vary somewhat for the various experimental points. As the yield curves are continued beyond π^{0} threshold, the next kinematically allowed process is $\gamma + D \rightarrow 2\pi + D$. The yield then continues to rise as the bremsstrahlung end point energy is increased, and this is the major background for η^{0} production. The curves clearly show the expected increase in deuteron yield corresponding to η^{0} productions. The arrows indicate the expected threshold energy at the center of the momentum acceptance. The yields show the expected behavior, which is a leveling off of the yield due to η^{0} production some 30-40 MeV above the threshold energy.

In order to determine the η^{0} differential cross sections from the measured yields, the height of the deuteron step must be determined, and this makes it necessary to extrapolate the two pion yields from below the η^{0} threshold where they are measured directly, to above the η^{0} threshold where the yields are the sum of an η^{0} signal and a two-pion yield. There is, also, of course, a constant contribution from π^{0} production. We have found that both pure phase space and a linear function are a good representation for the energy dependence of the data in the vicinity of the η^{0} threshold.

The actual interval which is fit is the region 100 MeV below the η^o threshold and a 100 MeV interval which starts 50 MeV above the η^o threshold. In figs. 3 and 4, the solid line is drawn in as a representation to the actual least squares curve. In this manner we obtain a least squares solution for the height of the η^o step.

The inserts in Figs. 3 and 4 show the deuteron yields in the vicinity of the η^o threshold with the background processes subtracted. These background processes include single π^o production, two-pion production, and a small ($\lesssim 10\%$) empty target background. If the background has been subtracted properly, the remaining yield will have the shape of a bremsstrahlung curve for fixed photon energy. The main feature of this curve is that the yield must plateau some 30-40 MeV above threshold. Figures 3 and 4 have this feature as do our other experimental points.

The η^o yields are converted into a differential cross section by normalizing to the deuteron yield where only π^o deuterons are produced, keeping the spectrometer momentum and angle fixed. We have then used the available differential cross section data for $\gamma + D \rightarrow \pi^o + D$ to normalize the data. These data are available at the appropriate photon energies but at lower momentum transfers. We have corrected these data to our momentum transfers using the shape of the measured deuteron electromagnetic form factors as obtained in Ref. 2.

We have measured such yield curves for 6 photon energies, which are in the laboratory frame: 668 MeV, 690 MeV, 708 MeV, 715 MeV, 722 MeV, and 776 MeV.The threshold energy for η^o production is 629 MeV. All points were taken near $\theta^*_{\eta^o} = 90^o$ in the c.m. system. The momentum transfers ranges from 564 MeV/c to 663 MeV/c.

RESULTS AND CONCLUSIONS

The interpretation of the results of this experiment are interesting primarily in relation to the process $\gamma + p \rightarrow \eta^{o} + p$. This reaction has been studied near threshold by the Stanford Group[1], and at somewhat higher energies by the Frascati and California Institute of Technology groups[3]. The rapid rise near threshold together with the information that the angular distribution near threshold is isotropic, show that the production is in an $S_{\frac{1}{2}}$ or $P_{\frac{1}{2}}$ state or a mixture of the two. Related experiments in the reaction $\pi^{-} + p \rightarrow \eta^{o} + n$ near threshold shows a similar behavior.[4] Recent theoretical considerations[5] have pointed out that the threshold behavior may be identified with a $T = \frac{1}{2}$ S wave resonance with mass $\simeq$ 1550 MeV which has been identified in pion nucleon scattering as a resonance with a high degree of inelasticity.

The process $\gamma + D \rightarrow \eta^{o} + D$ may be related to $\gamma + p \rightarrow \eta^{o} + p$ and $\gamma + n \rightarrow \eta^{o} + n$ within the frame work of the impulse approximation. A decomposition of the photoproduction amplitude may be made into an isoscalar and isovector component viz., $T = T^{o} + \tau_{3} T^{+}$ where T^{o} is the isoscalar and T^{+} the isovector part of the amplitude, and τ_3 is the z component of the nucleon isospin operator. Thus the amplitude for $\gamma + p \rightarrow \eta^{o} + p$ is $T^{o} + T^{+}$ and for $\gamma + n \rightarrow \eta^{o} + n$ it is $T^{o} - T^{+}$. For the process $\gamma + D \rightarrow \eta^{o} + D$ only T^{o} contributes. In the impulse approximation $\langle \eta^{o} D | T | \gamma D \rangle = \int d^{3}r \, e^{i \underset{\sim}{q} \cdot \underset{\sim}{r}/2} \, \psi_{d}(r) [T_{1}^{o} + T_{2}^{o}]_{AV.} \psi_{d}(r)$ where q is the laboratory deuteron recoil, r is the nucleon relative coordinate, and $\psi_{d}(r)$ is the deuteron ground state wave function. The amplitude $[T_{1}^{o} + T_{2}^{o}]_{AV.}$ represents an average over the deuteron Fermi momentum distribution for the single nucleon amplitudes. This has the effect of averaging over a range of photon energies. For a non-relativistic treatment of a final state $S_{\frac{1}{2}}$ or $P_{\frac{1}{2}}$ this reduces to:

$$|\langle\eta^{o}D|T|\gamma D\rangle|^{2} = 8/3\ |T^{o}|^{2}_{AV.} F^{2}(q^{2})$$

where $F^{2}(q^{2})$ is the deuteron electromagnetic form factor as defined in ref. (2). We have further assumed change independence for the η^{o} - nucleon coupling and neglected the small phase shifts due to an η^{o}-nucleon final state interaction. For comparison, the corresponding amplitude for production from single nucleons is: $|\langle\eta^{o}N|T|\gamma N\rangle|^{2} = |T^{o} + \tau_{3}T^{+}|^{2}$. Thus, a comparison of $\gamma + p \rightarrow \eta^{o} + p$ and $\gamma + D \rightarrow \eta^{o} + D$ can in principle determine the relative amounts of isoscalar and isovector in the amplitude.

For comparison of the two processes at the same c.m. final state momentum we thus have:

$$\frac{\left.\frac{d\sigma}{d\Omega^{*}}\right|_{\eta^{o}D}}{\left.\frac{d\sigma}{d\Omega^{*}}\right|_{\eta^{o}p}} \simeq \frac{(8/3\ |T^{o}|^{2}_{AV.} F^{2}(q^{2})}{|T^{o} + T^{+}|^{2}}$$

In Fig. 5, the differential cross section $\left.\frac{d\sigma}{d\Omega^{*}}\right|_{\eta^{o}D}$ is plotted as a function of p*, the meson c.m. momentum. All points have been normalized to the value of the deuteron form factor evaluated at $q^{2} = (2.98)^{2}\ F^{-2}$.

The features of interest are the rapid rise near threshold and the fall off with increasing c.m. momentum. This is very similar to the gross features seen in $\gamma + p \rightarrow \eta^{o} + p$. If Fig. 6 we have plotted $\frac{\left.\frac{d\sigma}{d\Omega^{*}}\right|_{\eta^{o}D}}{8/3\ F^{2}(q^{2})}$

and have also shown the Stanford results of the earlier experiment of $\gamma + p \rightarrow \eta^{o} + $] near threshold. The conclusions of interest are:

1. The simple picture of comparing the $\eta^{o}D$ and $\eta^{o}p$ experiments shows that the isovector part of the η^{o} photoproduction amplitude is small and consistent with zero.

2. There is approximately complete constructive interference between the η^{o}-proton and η^{o}-neutron amplitudes thus showing that the η^{o}-neutron and η^{o}-proton amplitudes have the same phase. This is consistent with the isoscalar character of the eta meson.

REFERENCES

1. R. Prepost, D. Lundquist, and D. Quinn, Phys. Rev. Letters 18, 82 (1967).
2. J. I. Friedman and H. W. Kendal, Phys. Rev. 129, 2802 (1963).
3. C. Bacci et al, Phys. Rev. Letters 16, 157 (1966); C. A. Heusch, C. Y. Prescott, E. D. Bloom, and L. S. Rochester, Phys. Rev. Letters 17, 573 (1966).
4. F. Bulos et al, Phys. Rev. Letters 13, 486 (1964); W. B. Richards et al, Phys. Rev. Letters 16,1221 (1966).
5. A complete set of references on this matter is given in Ref. 1.

FIGURE CAPTIONS

Fig. 1 Experimental arrangement for the experiment $\gamma + D \rightarrow \eta^{o} + D$.

Fig. 2 A typical time of flight distribution showing both a proton and deuteron peak.

Figs. 3 and 4 Two typical deuteron yield curves showing a signal due to η^{o} production. The inserts in the upper left corner show the yields in the vicinity of η^{o} threshold with backgrounds subtracted.

Fig. 5 The differential cross section for the process $\gamma + D \rightarrow \eta^{o} + D$ in the c.m. system versus p*, the c.m. final state momentum. The c.m. meson angle is $\simeq 90^{o}$.

Fig. 6 The differential cross section for $\gamma + D \rightarrow \eta^{o} + D$ divided by $8/3\ F^{2}(q^{2})$ versus p^{*}. The measured cross sections for the reaction $\gamma + p \rightarrow \eta^{o} + p$ with $\theta^{*}_{30} \simeq 90^{o}$ are shown for comparison purposes.

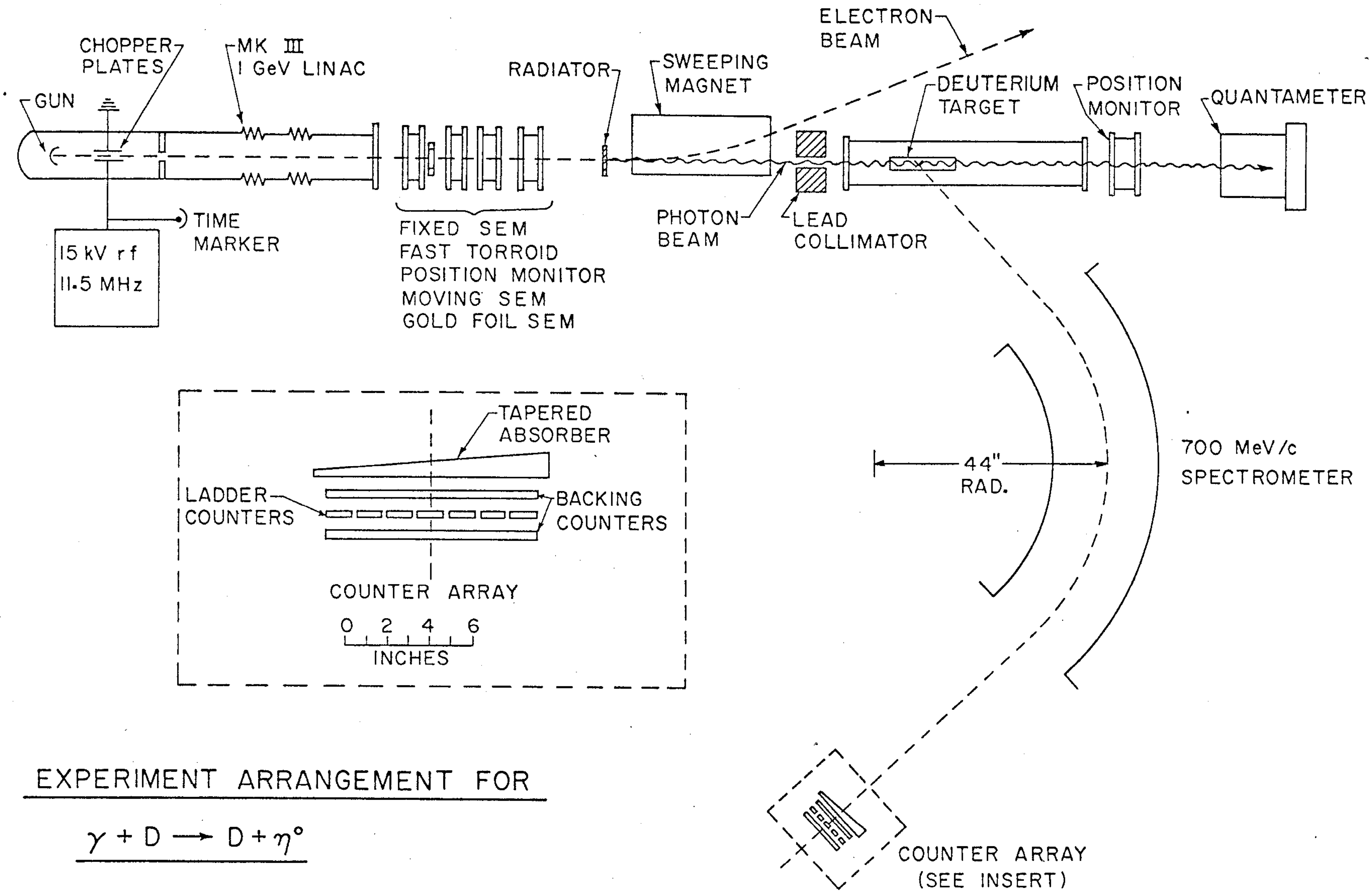

EXPERIMENT ARRANGEMENT FOR

$\gamma + D \longrightarrow D + \eta^{\circ}$

FIG. 1

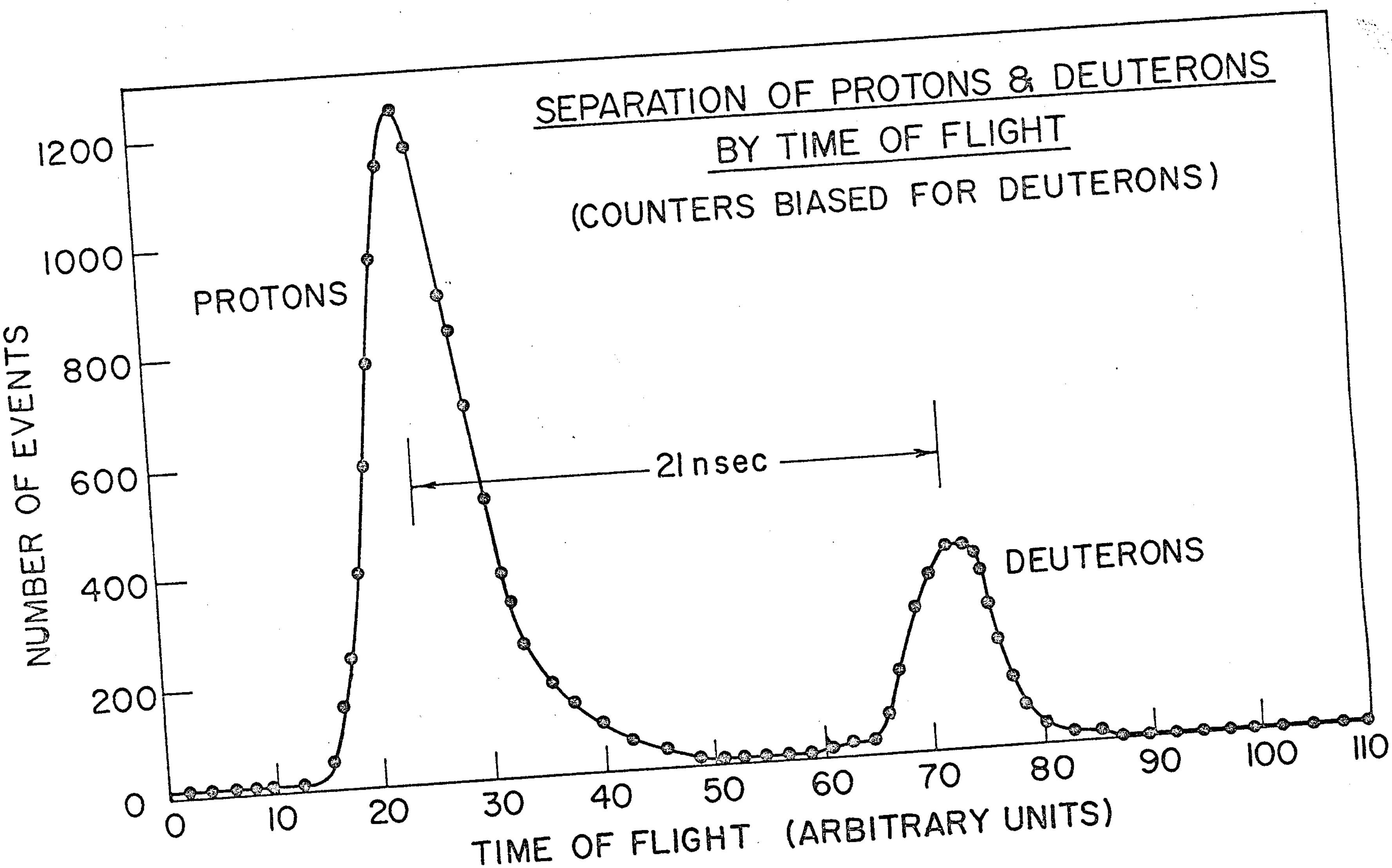
SEPARATION OF PROTONS & DEUTERONS
BY TIME OF FLIGHT
(COUNTERS BIASED FOR DEUTERONS)
NUMBER OF EVENTS
1200
1000
800
600
400
200
0
PROTONS
21 nsec
DEUTERONS
0
10
20
30
40
50
60
70
80
90
100
110
TIME OF FLIGHT (ARBITRARY UNITS)

FIG. 2

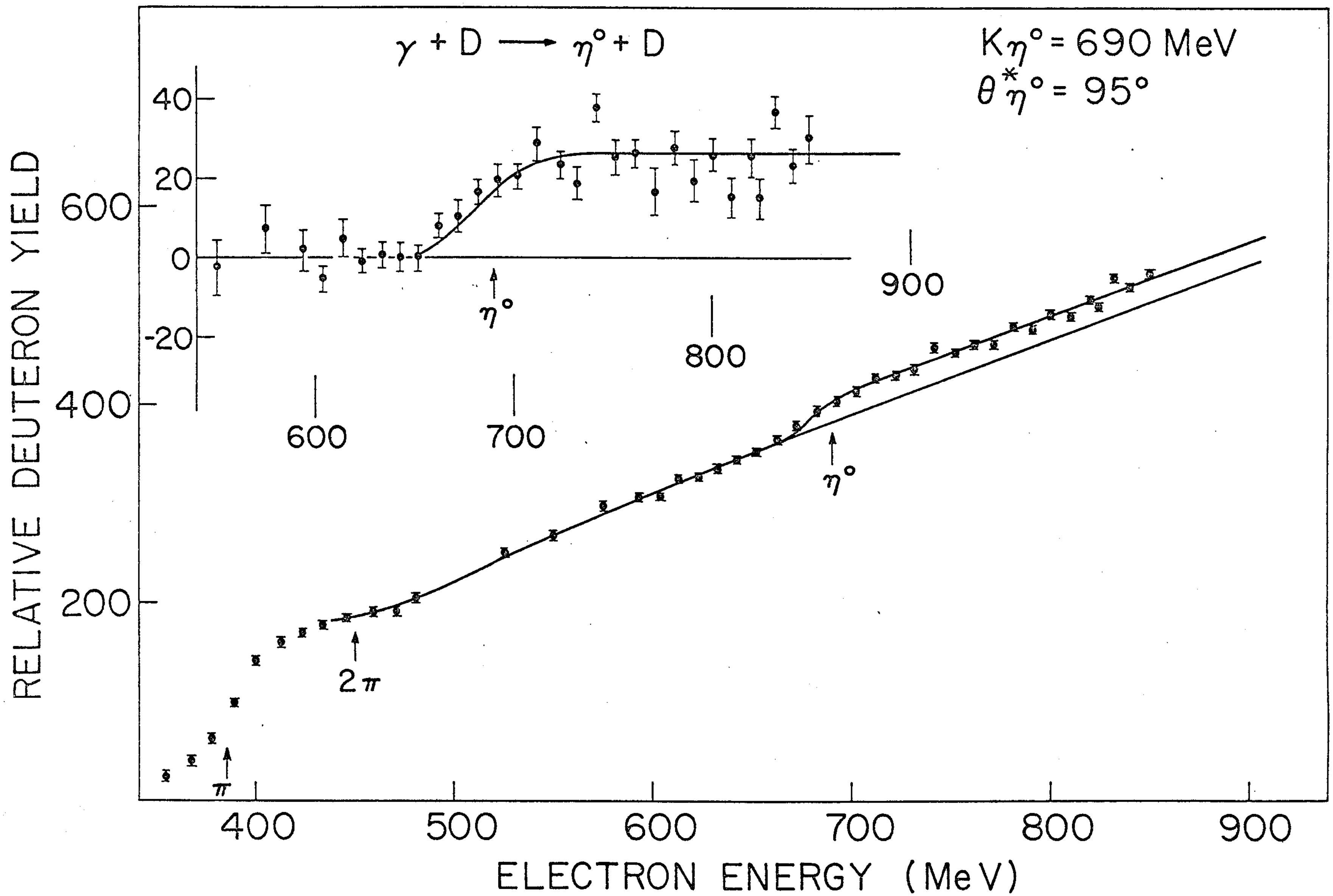

γ + D → η° + D
Kη° = 690 MeV
θ*η° = 95°
RELATIVE DEUTERON YIELD
ELECTRON ENERGY (MeV)
40
20
0
-20
600
700
800
900
η°
2π
π
200
400
600
400
500
600
700
800
900

FIG. 3

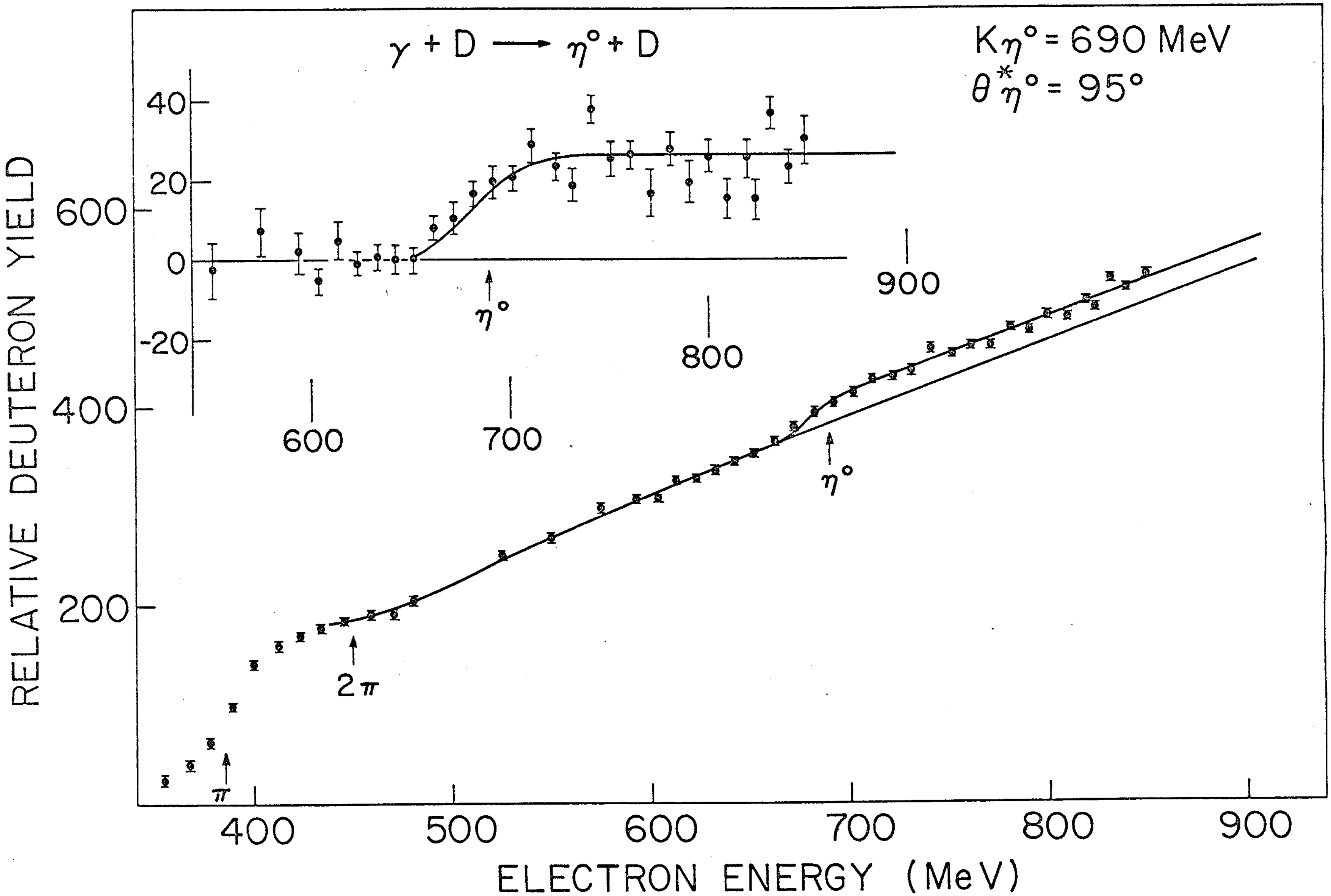

γ + D ⟶ η° + D
Kη° = 690 MeV
θ*η° = 95°
RELATIVE DEUTERON YIELD
ELECTRON ENERGY (MeV)
40
20
0
-20
600
700
800
900
η°
600
400
200
π
2π
η°
400
500
600
700
800
900

FIG. 4

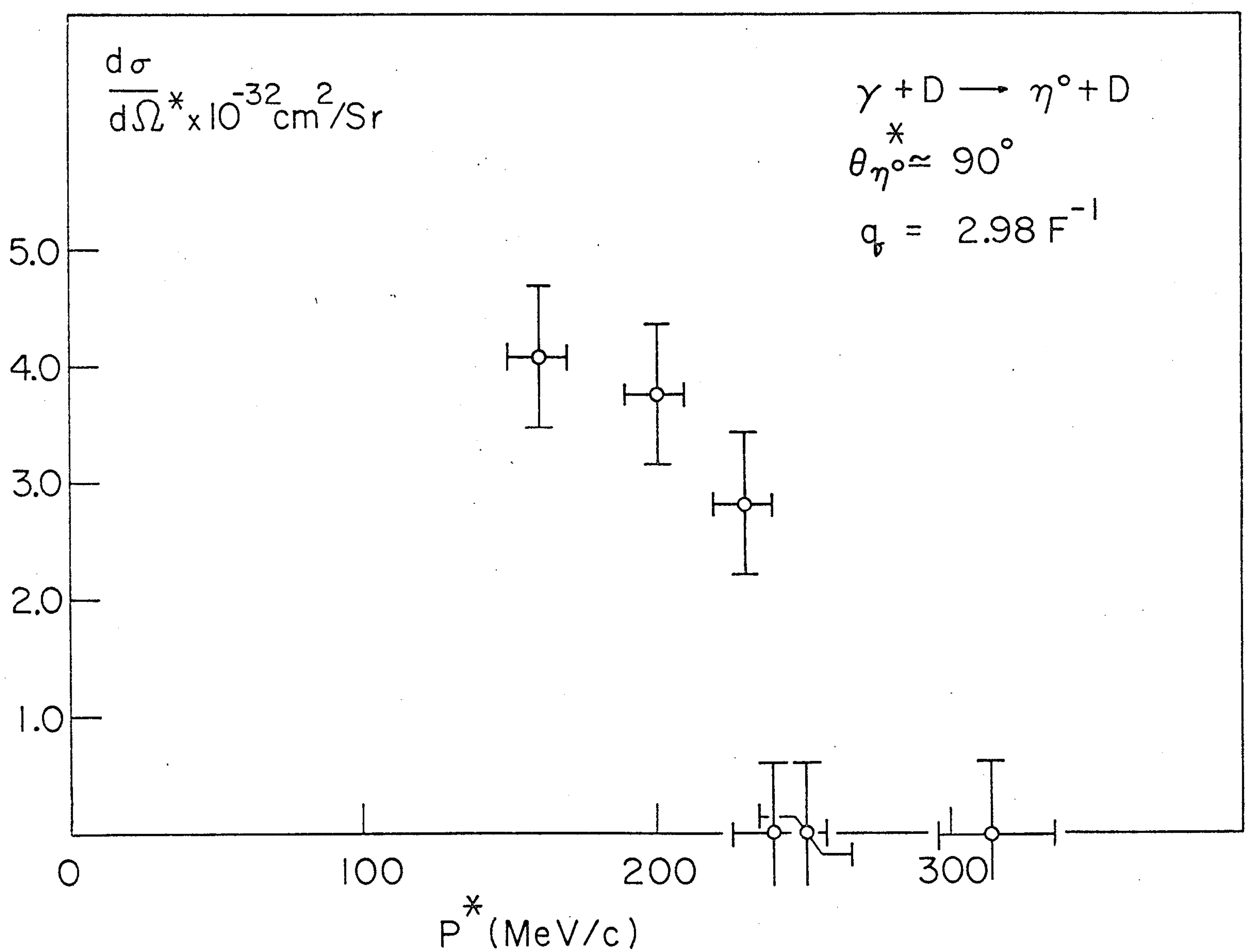

$\frac{d\sigma}{d\Omega^*} \times 10^{-32} cm^2/Sr$
$\gamma + D \longrightarrow \eta^\circ + D$
$\theta^*_{\eta^\circ} \simeq 90^\circ$
$q_\gamma = 2.98\ F^{-1}$
5.0
4.0
3.0
2.0
1.0
0
100
200
300
P^* (MeV/c)

FIG. 5

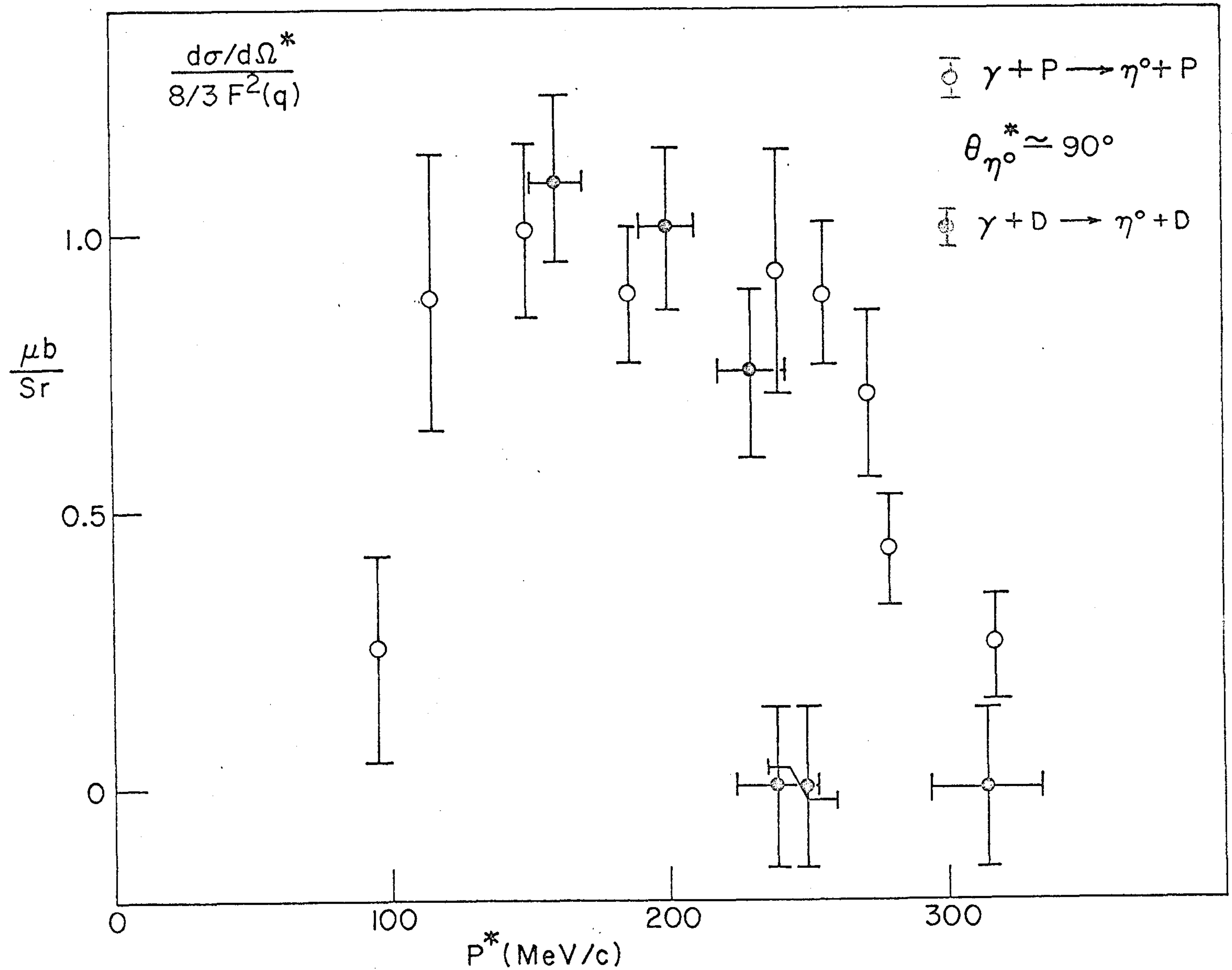

$\frac{d\sigma/d\Omega^*}{8/3\,F^2(q)}$
$\gamma + P \longrightarrow \eta^\circ + P$
$\theta_{\eta^\circ}^* \simeq 90^\circ$
$\gamma + D \longrightarrow \eta^\circ + D$
1.0
0.5
0
$\frac{\mu b}{Sr}$
0
100
200
300
P^*(MeV/c)

FIG. 6